Journal of Materials Chemistry C

ROYAL SOCIETY OF CHEMISTRY

PAPER

View Article Online
View Journal | View Issue

Check for updates

Cite this: J. Mater. Chem. C, 2022, 10, 12012

Luminescent assemblies of pyrene-containing bent-core mesogens: liquid crystals, π-gels and nanotubes†

Marta Martínez-Abadía, ‡[a] Shinto Varghese, §[b] Johannes Gierschner, *[b] Raquel Giménez *[a] and M. Blanca Ros *[a]

Bent-shaped molecules incorporating terminal pyrene moieties were designed and synthesized aiming at promoting a variety of luminescent self-assembled materials. The novel compounds are fluorescent both in solution and in condensed phases, achieving brighter fluorescence in the last case with fluorescence quantum yields up to 60%. Depending on the number of pyrene units (1 or 2) and/or the presence or absence of a long and flexible linker between the bent-core and the pyrene structures, bent-core liquid crystal phases, physical gels and nanoassemblies were obtained. Their properties depend on the molecular design, unveiling a synergistic and versatile 'tandem' of the bi-functional system in supramolecular functional materials chemistry. Long hydrocarbon spacers connecting bent-core and pyrene structures were necessary to display mesomorphic properties, achieving monotropic rectangular columnar mesophases, being for one compound stable at room temperature and displaying a glassy transition below room temperature, as revealed by POM, DSC and XRD. Liquid crystal phases exhibited excimer-like emission. In addition, organogels were obtained without the help of hydrogen bonding functionalities, exhibiting in one case supergelator behavior. Different nanoassemblies were obtained from these non-amphiphilic bent-core structures, in particular unprecedented organic nanotubes with beveled ends formed by a single bilayer.

Received 17th June 2022,
Accepted 26th July 2022

DOI: 10.1039/d2tc02546a

rsc.li/materials-c

Published on 29 Julai 2022. Downloaded on 30/01/2026 1:59:07 PTG.

Introduction

Pyrene is a well-known organic chromophore that possesses remarkable photophysical and electronic properties,[1–5] as well as very attractive supramolecular capabilities.[4–9] This polycyclic aromatic hydrocarbon combines the high fluorescence quantum yield of the monomer in solution and aggregated states, and efficient excimer emission for integration into devices such as OLEDs.[3] In addition, it is highly sensitive towards micro-environmental changes,[10] being extensively used as probes either for biological purposes[11] to obtain structural and dynamic information on multi-molecular assemblies,[12–14] or for photonic devices.[15–18]

To achieve in these targets, two key features have been observed to be essential for modulating the functional performance and processability, namely appropriate molecular design and organization of the active motifs. Therefore, a variety of pyrene-containing molecular structures, suitable for supramolecular arrangements, have been reported with the aim of self-organizing the pyrene moiety.[3] By using both intra- and intermolecular interactions, a number of strategies and bottom-up methodologies have been proposed to achieve the desired functional properties.[6–14] Thus, non-covalent interactions, including π–π stacking, van der Waals forces and hydrogen-bonds, among others, are crucial to obtain programmed molecular building blocks that evolve into well-defined hierarchical responsive superstructures.[15–18] In this regard, physical gels and liquid crystalline phases have attracted special attention. Gels,[9,14,19–22] through the spontaneous aggregation of pyrene-based small molecules or polymers as gelators, assemble into 1D fibrils that are further entangled into a complex 3D network, in which a large amount of solvent can be immobilized. The so-called π-gels[23,24] can potentially provide the structural control required for low-cost and large-area liquid deposition methods.

[a] Instituto de Nanociencia y Materiales de Aragón (INMA), Departamento de Química Orgánica-Facultad de Ciencias, Universidad de Zaragoza-CSIC, E-50009 Zaragoza, Spain. E-mail: bros@unizar.es, rgimenez@unizar.es

[b] Instituto Madrileño de Estudios Avanzados en Nanociencia (IMDEA Nanociencia), Ciudad Universitaria de Cantoblanco, E-28049, Madrid, Spain. E-mail: johannes.gierschner@imdea.org

† Electronic supplementary information (ESI) available. See DOI: https://doi.org/10.1039/d2tc02546a

‡ Present address: POLYMAT, University of the Basque Country UPV/EHU, Avenida de Tolosa 72, E-20018 Donostia–San Sebastian, Spain.

§ Present address: School of Applied & Interdisciplinary Sciences, Indian Association for the Cultivation of science, 2A & 2B, Raja S.C. Mullick Road, Kolkata-700032, West Bengal, India.

This journal is © The Royal Society of Chemistry 2022

Published on 29 Julai 2022. Downloaded on 30/01/2026 1:59:07 PTG.

On the other hand, liquid crystals[25–27] have provided a variety of classical layered or columnar anisotropic functional self-assemblies, also incorporating pyrene units,[28–38] providing a control over their organization that determines their optical and electronic properties. However, only a few suitable molecular design strategies providing both types of soft materials in the route to versatile functional materials have been published.[39–48]

Concerning mesophase organizations, bent-core liquid crystals (BCLCs), which were discovered around 1996,[49] and their non-conventional mesophases have received significant attention in the soft matter area in the last decades.[50–57] Their compact packing has allowed the development of novel liquid crystal phases with polar and in certain cases chiral arrangements, providing materials with very attractive functional properties.[54,56,58–61] Ferro- and antiferroelectric switching, piezoelectric or nonlinear optical responses from their polar molecular non-centrosymmetric order, have been reported even by using achiral molecules. Additionally, limited but striking luminescent bent-core type mesophases have also been afforded.[62–70] Interestingly, the combination of properties such as polarity, supramolecular chirality and luminescence endows bent-core liquid crystal phases with challenging opportunities in the context of chiral nanoarchitectonics.[71–73]

Efficient strategies to increase the potential for supramolecular arrangements of bent-core molecules have been developed by the incorporation of different structural motifs in the same bent-shaped molecule. For this purpose, the use of dimers,[74] dendrimers[75,76] or hybrid molecules including bulky Si-containing moieties[77–81] or C60-units[82,83] has been successful, paving the way to the possibility of stabilizing, even at room temperature, certain soft supramolecular order and obtaining interesting physical properties by controlling the nano-segregation and polar orientation of bent-core moieties.

Attractively, in the last few years some authors have reported[48,84,85] that the compact packing of bent-shaped structures, which promotes BCLCs, also occurs in the presence of a poor solvent, providing products ranging from single objects to supramolecular gels and, consequently, greatly increasing the potential of bent-core molecules and attracting academic and applied materials science interests.

Based on all these results and perspectives, we were attracted by the combination of bent-core molecules with the luminescent pyrene units. Thus, innovative and challenging designs of new photoactive functional materials and fluorescent probes for mesophase characterization could be proposed, and the potential of the new pyrene-bent core building blocks could be explored to provide self-assembled materials displaying BCLC-like features at room temperature.

Herein, the supramolecular abilities of five bent-shaped molecules that incorporate the pyrene structure are analyzed aiming at promoting both bent-core liquid crystalline phases and supramolecular gels (Fig. 1). In order to design bent-shaped molecules and induce BCLCs, the well-known 3,4'-biphenylene system was selected as the central core. These compounds differ in the number of 1-pyrenebutyrate (Pyb) units (1 or 2) and in the presence or absence of a long and flexible linker between the bent-core structure (B) and the Pyb motif. Two bent-shaped di-pyrenebutyrate compounds, named Pyb-0-B-0-Pyb and Pyb-11-B-11-Pyb, without a spacer (0) and with a spacer of 11 carbon atoms, respectively; two mono-substituted ones, Pyb-0-B and Pyb-11-B, as well as one product where the Pyb unit was replaced by 1-pyrenebutyramide (PybN), PybN-11-B, were synthesized and characterized. To examine the role of pyrene units and their proximity to the bent-core structure in the formation of bent-core mesophases and gels, and also to assess the photoluminescence of these new supramolecular materials by studying the UV-Vis absorption and fluorescence are the main targets of our study.

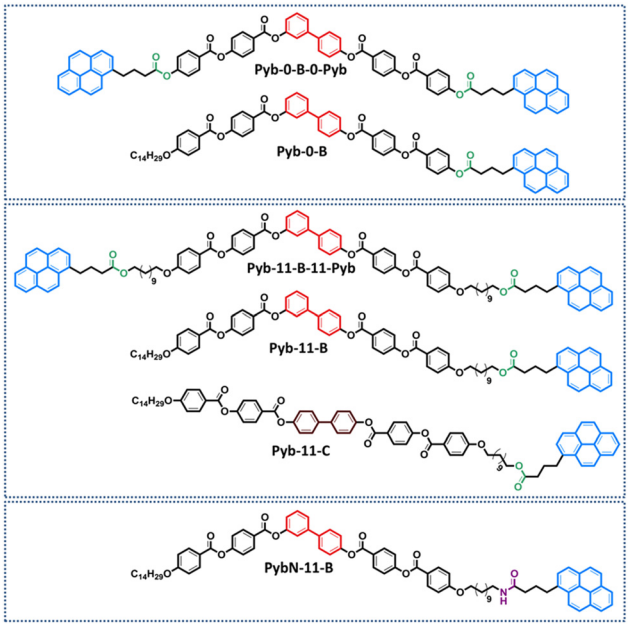

Fig. 1 Chemical structures of the bent-shaped and rod-like pyrene derivatives.

In addition, to analyzed the key role of a bent structure in these supramolecular trends and properties, a rod-like molecule, namely Pyb-11-C (C denotes the calamitic structure), has been incorporated in this structure–property relationship study.

Results and discussion

Synthesis

The synthetic methods for the preparation of pyrenebutyrate and pyrenebutyramide derivatives are shown in Schemes S1–S6 in the ESI.† The synthetic routes have been adapted from studies on similar intermediates and are based on Mitsunobu reactions and successive esterification and deprotection of benzyl groups. All experimental details and structural characterization of the compounds are described in the ESI.†

Thermal and liquid crystalline properties of the compounds

The phase transitions of the final target compounds were studied by polarizing optical microscopy (POM), differential scanning calorimetry (DSC) and X-ray diffraction (XRD). The

Published on 29 Julai 2022. Downloaded on 30/01/2026 1:59:07 PTG.

transition temperatures, enthalpies and XRD data are collected in Table 1.

As it can be seen, only Pyb-11-B-11-Pyb, Pyb-11-B and Pyb-11-C, all with a long spacer, exhibit liquid crystalline properties. Regarding bent-core compounds, Pyb-11-B was obtained as a crystal with a melting point of 110 °C and exhibits a mesophase in the cooling process with a spherulitic and pseudo focal-conic texture (Fig. 2). Pyb-11-B-11-PyB shows a lower melting point and also a monotropic mesophase but with a different behaviour, as the liquid crystal phase remains stable without crystallizing during the following heating/cooling cycles and it shows a glass transition below room temperature. The diffraction patterns of mesophases for Pyb-11-B-11-Pyb and Pyb-11-B show several sharp reflections in the small angle region that do not correspond to lamellar structures, but can be attributed to a bent-core columnar mesophase with a rectangular unit cell (Col_r) (Fig. 2).

Considering the planarity of the pyrene unit that tends to be stacked with other pyrenes, and the close packing observed in BCLCs, significantly higher transition temperatures for these pyrene-bent-core derivatives than those for the analogous bent-core compounds without pyrene-butyrate units would be expected. However, slightly lower melting points and enantiotropic liquid crystalline mesophases have been reported for bent-compounds without the pyrene groups,[86,87] while for the bent-core compounds studied here mesomorphism is not stabilized after melting. Only in the cooling process from the isotropic liquid with higher molecular mobility, interactions can stabilize mesomorphism, but only in molecules with long flexible linkers connecting bent-core structures and the pyrene unit. This is in good agreement with the reported data, revealing the essential role of long terminal tails in stabilizing the bent-core mesophase, while short chains favor solid phase formation. Furthermore, when long spacers connect bent-core and pyrene structures, the conformational freedom of the lengthy tails could both partially prevent the tendency of the pyrene to stack up in order to induce monotropic columnar phases, as well as to wrap them between the hydrocarbon chains, dispersing the pyrene units and weakening the intermolecular interactions. Thus, this structural tandem, long flexible linkers and the pyrene unit, seems to distort the pyrene packing as will be supported later by photo-physics studies.

In contrast, the rod-shaped compound Pyb-11-C melts above 155 °C and forms an enantiotropic SmC mesophase in a broad range of temperatures (around 100 °C) (Fig. S7, ESI†). The diffraction pattern exhibits two reflections at a small angle, which are assigned to (001) and (002) of lamellar packing, which allows us to calculate a spacing layer (43.5 Å) much lower than the theoretical molecular length (85.1 Å), suggesting the molecular tilt inside the smectic layer.

The linear structure allows larger π-stacking and van der Waals interactions, indicated by the high melting points and clearing. These strong contacts can allow segregation between the central structures and the terminal chains, which would indicate high tilt angles, approaching 31°, rather common in biphenyl-based liquid crystals[54] and the different behavior observed here between the bent-core and linear compounds.

Table 1 Thermal properties and XRD liquid crystal characterization data for the target compounds

Compound	Phase transition T (°C) [ΔH (kJ mol^{-1})][ab]	Mesophase (T (°C) of XRD data)	d (Å)	Miller index (hkl)	Parameters (Å)
Pyb-0-B-0-Pyb	Cr 168 [41.1][c] I I 143 [34.8] Cr Cr 168 [32.9][c] I	—	—	—	—
Pyb-11-B-11-Pyb	Cr 90 [76.2][c] I I 69 [8.6] Col_r 6[d] Col_{rg} Col_{rg} 8 Col_r 75[d] [8.7] I	Col_r (rt)[f]	57.8 29.8 24.3 19.3	101 002 602 303	a = 230.3 c = 59.7
PyB-0-B	Cr 146 [45.1][c] I I 111 [36.9] Cr Cr 145 [38.9][c]	—	—	—	—
Pyb-11-B	Cr 110 [76.2][c] I I 103 [14.7] Col_r 65 [29.1] Cr Cr 110 [68.4] I	Col_r (102)	44.8 29.0 22.7	101 002 202	a = 73.9 c = 56.4
PybN-11-B	Cr 165 [60.1] I I 143 [60.5][c] Cr Cr 164 [58.2] I	—	—	—	—
Pyb-11-C	Cr 158[c] [48.9] SmC 250[e] Dec SmC 154[d] [48.6] Cr Cr 157 [48.4] SmC 250[e] Dec	SmC (168)	43.5 21.8	001 002	c = 43.5

[a] Data determined by DSC. Temperatures at the maximum of the peaks from the first heating and cooling and the second heating cycle at a scanning rate of 10 °C min^{-1}. Cr: crystal phase, SmC: smectic C mesophase, Col_r: rectangular columnar mesophase, Col_{rg}: vitrified rectangular columnar mesophase, I: isotropic liquid. [b] The crystal phase denoted as Cr is, in most cases, not unique (crystalline polymorphism). [c] Combined enthalpy of several crystalline transitions. [d] Onset data. [e] Data obtained from POM. [f] Measured at room temperature (rt) by cooling the sample quickly from the isotropic liquid.

 This journal is © The Royal Society of Chemistry 2022

Published on 29 Julai 2022. Downloaded on 30/01/2026 1:59:07 PTG.

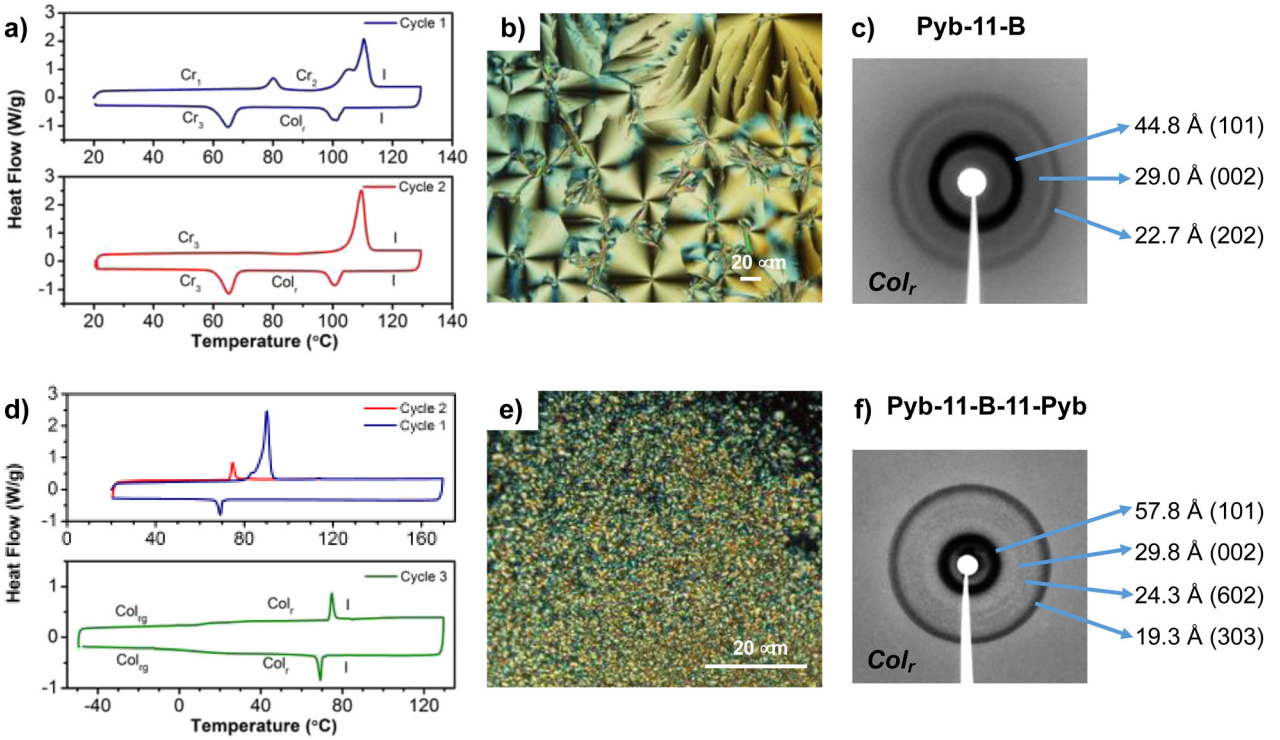

Fig. 2 DSC thermograms and first and second heating/cooling cycles of Pyb-11-B (a) and Pyb-11-B-11-Pyb (d); POM textures of Pyb-11-B at 104 °C (Col$_r$ phase) (b) and Pyb-11-B-11-Pyb at 74 °C (Col$_r$ phase) (e); and XRD patterns of the mesophases of Pyb-11-B, Col$_r$ phase at 102 °C, (c) and Pyb-11-B-11-Pyb, Col$_r$ phase at room temperature (f).

Photo-physics in solution and in the solid and liquid crystalline states

The UV-Vis absorption spectra in dichloromethane (DCM) solution of these compounds exhibit distinct absorption bands. The sharp features in the 300–350 nm region correspond to the vibronics of the $S_0 \rightarrow S_2$ transition of pyrene,[88] and those $<$280 nm to higher excited states of pyrene; the unstructured shoulder in the 280–300 nm region is assigned to biphenyl absorption of the angular bent-core (or rod-core) structure (Fig. 3a, Table 2 and Table S1, ESI†). Regardless of the spacer, the absorption spectra of the compounds with a single pyrene unit are similar in the spectral range above 300 nm, while in those with two pyrene units the pyrene absorption characteristics roughly doubles. The fluorescence spectra of all compounds in dilute DCM solution exhibit vibronically structured monomer emission (Fig. 3b), originating from the relaxed S_1 state of pyrene, with a maximum at 377 nm, and side bands at 397 and 418 nm of vibronic origin. The fluorescence quantum yields were measured in solutions in air and the values were around 13–16% (Table 2).[89]

In the condensed state of the compounds, the fluorescence was evaluated in different phases: the as-obtained solid (identified as pristine), processed solids, *i.e.* films cooled down from the mesophase at 10 °C min^{-1} (identified as scf), and liquid crystal phases (identified as LC or mesophase). In all pristine, scf and mesophase spectra, excimer formation is observed, characterized by a broad, unstructured emission which peaks at about 478 nm (see Fig. 3 and Fig. S8, ESI†); in fact, in most cases, the excimer emission dominates the spectra (see Table S2, ESI†). Since dynamic excimer formation, as

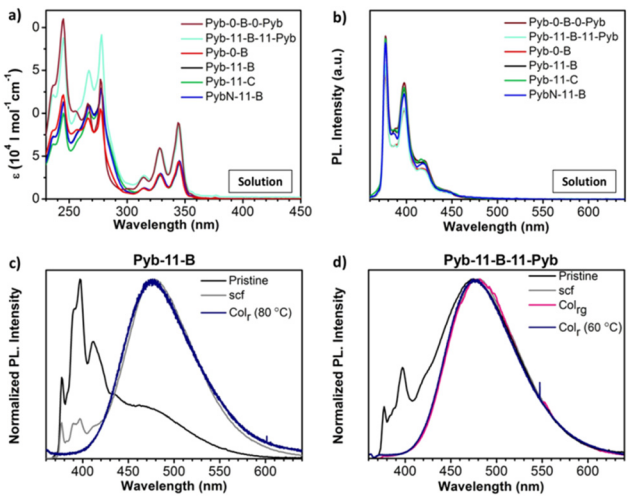

Fig. 3 (a and b) Absorption and fluorescence spectra, respectively, of the final compounds in dichloromethane (DCM) solutions (see also Table 2). The original fluorescence spectra have been divided by absorbance at the excitation wavelength for better comparison. (c and d) Fluorescence spectra in different neat film and mesophase samples of Pyb-11-B and Pyb-11-B-11-Pyb. Pristine powder (black), scf: slow cooled film at 10 °C min^{-1} (grey), Col$_r$: rectangular columnar mesophase (dark blue); and Col$_{rg}$: glassy rectangular columnar mesophase (pink).

Table 2 Photoluminescence data in dichloromethane (DCM) solution (in air) and the as-obtained solid (pristine): emission maxima (λ_{em}), fluorescence quantum yields (Φ_F) and lifetimes (τ_F), and radiative and non-radiative rates (k_r, k_{nr})

	DCM solution		As-obtained solid (pristine)				
Compound	λ_{em} (nm)	Φ_F [a]	λ_{em} (nm)	Φ_F [b]	τ_F [c] (ns)	k_r [d] (s^{-1})	k_{nr} [d] (s^{-1})
Pyb-0-B-0-Pyb	377	0.16	478	0.58	94.4	6.1×10^6	4.4×10^6
Pyb-11-B-11-Pyb	377	0.13	475	0.55	57.0	9.6×10^6	7.9×10^6
PyB-0-B	377	0.13	476	0.60	42.9	1.4×10^7	9.3×10^6
Pyb-11-B	377	0.14	377, 391, 397, 412	0.59	53.1	1.1×10^7	7.3×10^6
PybN-11-B	377	0.14	449	0.19	16.2	1.2×10^7	5.0×10^7
Pyb-11-C	377	0.15	470	—	—	—	—

[a] From relative measurements using 9,10-diphenylanthracene in cyclohexane as a reference (Φ_F = 0.9). [b] From absolute measurements in an integrating sphere. [c] Intensity averages from bi- and tri-exponential fits (see Table S3, ESI). [d] From $\tau_F = 1/(k_r + k_{nr})$, $\Phi_F = k_r \cdot \tau_F$.

Published on 29 Julai 2022. Downloaded on 30/01/2026 1:59:07 PTG.

observed in solution,[2] can be excluded for the condensed phases, it can be concluded that the pyrenes generally stack in the condensed phases. In the ampler definition by Birks, also such ground state complexes of pyrene are considered as excimers.[90] For all mesophases, exclusive excimer emission is observed (see Fig. 3 and S8, ESI†), indicating regular short-range order with pronounced π–π stacking of the pyrene units. Very pronounced excimer formation is also found for the pristine and the thermally treated samples (scf) (see Fig. 3 and Fig. S8, Table S2, ESI†), pointing to similar short-range interactions with respect to the mesophases of the materials.

A notable exception is Pyb-11-B, which shows significant monomer emission in the pristine state (~65% of the total fluorescence intensity; see Fig. 3c and Table S2, ESI†), giving rise to dual emission;[91] here, the monomer peak corresponds to that observed in solution (Fig. 3a). Under thermal treatment the excimer content increases to 94%, and in the columnar mesophase only excimer emission is observed (see Fig. 3c).

Some monomer emission is observed also in pristine Pyb-11-B-11-Pyb (~8%) (Fig. 3d), which however disappears in the scf and mesophase. This result gives further evidence to our proposed scenario, that, when long spacers connect bent-core and pyrene structures, the intermolecular interactions significantly distort the pyrene packing. However, this is not the case for the 1-pyrenebutyramide compound, PybN-11-B (Fig. S8g, ESI†), showing an excimer emission in all solid phases, being however blue-shifted by ~30 nm with respect to the excimer bands of the other compounds. Most probably, this is associated to a different arrangement of the pyrene units due to a competitive/cooperative intermolecular H-bonding and π–π interaction balance.[31,92] In fact, the excimer band shape and spectral position (as well as intensity) are expected to be very sensitive to the precise position (separation, lateral displacement, rotation) of adjacent π-stacked molecules.[93–96]

Remarkably, the fluorescence quantum yields Φ_F of the pristine films of the 1-pyrenebutyrate compounds are all high with values of *ca.* 60% (Table 2), despite excimer formation. In fact, excimers are often assumed to be little emissive due to the vanishing oscillator strength of the emissive state (resulting in a low radiative rate k_r).[97] However, the resulting Φ_F is always decided by the competition of k_r with the non-radiative rate k_{nr},[98] so that pyrene excimers can be highly emissive in the crystalline[99] and liquid crystalline states.[28] We therefore measured the excimer lifetimes, giving about 42–94 ns in the pristine state (see Table 2). The rate constant analysis (Table 2) reveals that k_r is indeed small with a value of *ca.* 1×10^7 s^{-1},[100] but can easily compete with k_{nr}, which is effectively suppressed in solid environments.[101] However, it should be noted that the excimer lifetimes exhibit a non-exponential behaviour (for details, see Table S3 and Fig. S9, ESI†),[102] which is ascribed to the slightly different geometrical arrangements of the pyrene excimers due to non-negligible disorder in the pristine samples. Finally, the pristine PybN-11-B excimer shows a much lower quantum yield (19%). This is however not due to a lower k_r (which is essentially the same as that in the other compounds), but due to a higher k_{nr}, indicating again a different and less restrictive environment in the case of the compound with the amide group.

Gelation properties and photo-physics in the gel state

Pyrene derivatives have been very often used to produce luminescent gels with different applications,[4,9,15,103–105] most of them mediated by hydrogen bonding.[4,15,23,106] On the other hand, few but consistent studies proved the ability of bent-core compounds as gelators.[48,84,107,108] In our case, the presence of an aromatic core (pyrene) and a bent-core structure prompted us to check their gelation abilities by π–π stacking in various polar or nonpolar, protic or aprotic solvents, namely 1-butanol, 1-octanol, toluene, nitrobenzene and chlorobenzene (see Table S4, ESI†). For gelation tests, the mixture was heated until the solid was completely dissolved and the resulting clear solution was cooled in air to room temperature. The gel formation criterion used was to verify the absence of the flow of the solution when the test tube was turned upside down at room temperature (see the ESI†). Due to the low solubility of the di-substituted compounds, Pyb-11-B-11-Pyb and Pyb-0-B-0-Pyb, in the selected solvents, we limited our study to the gelation properties of compounds with only one pyrene unit, Pyb-0-B, Pyb-11-B, PybN-11-B and Pyb-11-C.

Interestingly, Pyb bent-core derivatives are suitable gelators of aliphatic alcohols such as 1-butanol or 1-octanol, giving rise to opaque gels (Fig. 4c). Attractively, for this family of bent-shaped compounds, the presence of an amide group is not essential for the gelation. Moreover, the lowest critical gelation concentration (0.3% w/w) has been reached for compound Pyb-11-B, acting as a supergelator. In contrast, PybN-11-B only can gelate 1-octanol at higher concentrations (10% w/w), being,

 This journal is © The Royal Society of Chemistry 2022

Published on 29 Julai 2022. Downloaded on 30/01/2026 1:59:07 PTG.

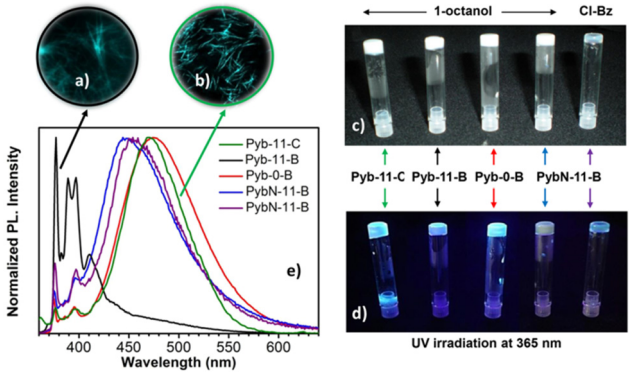

Fig. 4 Fluorescence microscopy images of the xerogels of Pyb-11-B (a) and Pyb-11-C (b) irradiated at 385–400 nm. Photographs of the gels of Pyb-11-B (10% w/w, black line), Pyb-0-B (10% w/w, red line), Pyb-11-C (5% w/w, green line), and PybN-11-B (10% w/w, blue line) in 1-octanol, and PybN-11-B (10% w/w, purple line) in chlorobenzene, all under room light (c) and UV light irradiation (d). Fluorescence spectra of the gels (e).

on the other hand, the only gelator for aromatic solvents such as nitrobenzene or chlorobenzene, leading to transparent gels (Fig. 4c). All these organogels exhibit thermally reversible sol-to-gel phase transitions; furthermore, upon UV irradiation, these gels exhibit strong luminescence (Fig. 4d), keeping the attractive optical features of the pyrene unit. Fluorescence microscopy allowed us to visualize the luminescent network (Fig. 4a and b).

Fluorescence measurements (Fig. 4 and Table S5, ESI†) show that the emission properties of the gels strongly depend on the chemical structure of the gelator, namely the length of the spacer and the nature of the linkage (ester *vs.* amide) connecting pyrene and bent-core moieties (Fig. 4e). In general, the gel emissions are similar to the optical properties evaluated for the pristine samples of gelators. In 1-octanol, all gels show excimer formation; an exception is again Pyb-11-B, which displays dual emission of the monomer and excimer bands similar to the as-obtained solid, but with different relative intensities.

Evidently, pyrene stacking is not sufficient to act as a driving force for gel formation; this is ascribed to the combination of the presence of only one pyrene unit and the long flexible spacer, which only partly allows for excimer formation. This supports our proposal to explain the poor liquid crystal properties and monomeric fluorescence of Pyb-11-B.

In contrast, through the participation of H-bonds promoting the stacking of pyrene moieties, PybN-11-B-based gels in 1-octanol exhibit also a blue-shifted excimer emission with a

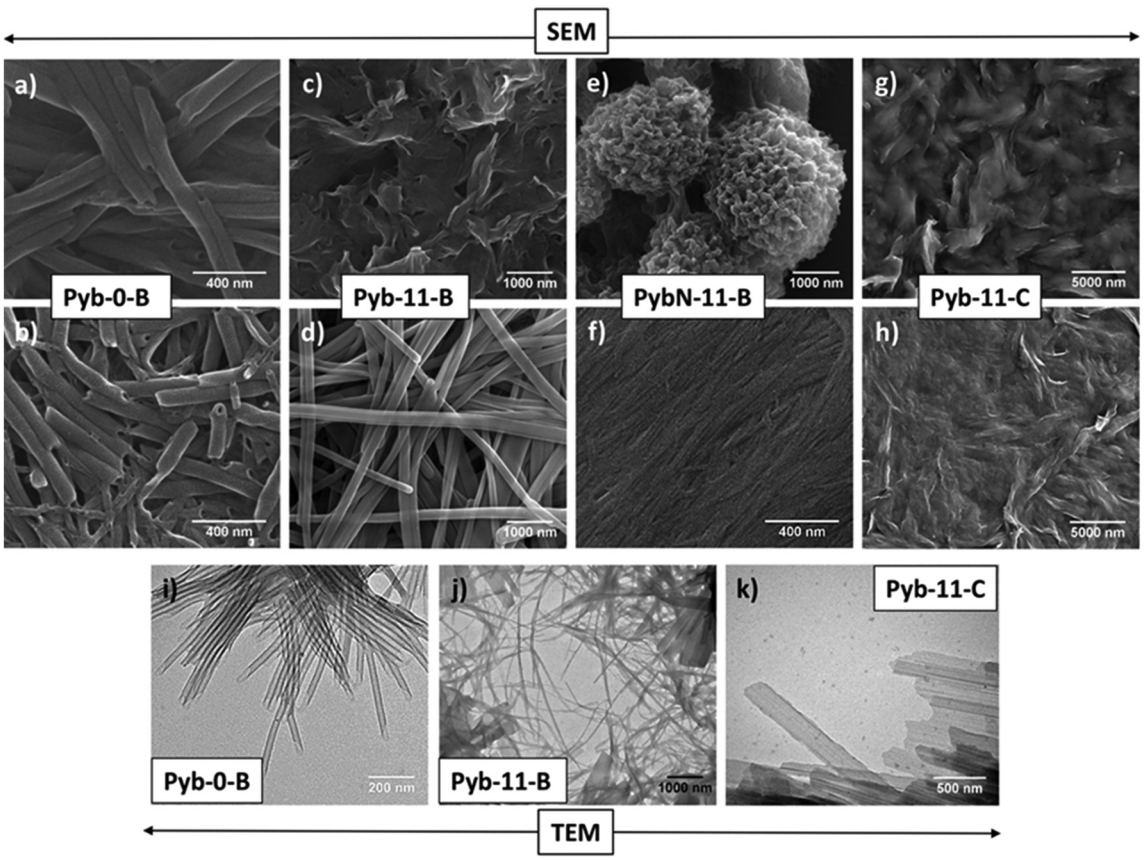

Fig. 5 SEM images of the xerogels of (a and b) Pyb-0-B in 1-octanol (10% and 2.5% w/w, respectively); (c and d) Pyb-11-B in 1-octanol (10% and 0.3% w/w, respectively); (e) PybN-11-B in 1-octanol (10% w/w); (f) PybN-11-B in chlorobenzene (10% w/w); and (g and h) Pyb-11-C in 1-octanol (5% and 0.8% w/w, respectively). TEM images of aggregates: (i) Pyb-0-B in 1-octanol (0.1% w/w); (j) Pyb-11-B in 1-octanol (0.1% w/w); and (k) Pyb-11-C in 1-octanol (0.2% w/w).

Published on 29 Julai 2022. Downloaded on 30/01/2026 1:59:07 PTG.

lower lifetime (Table S5 and Fig. S10, ESI†). The morphology of the network structure of the xerogels was examined by scanning electron microscopy (SEM). Fig. 5 shows the electron micrographs of the xerogels deposited on glass slides from different gels in 1-octanol and in chlorobenzene for PybN-11-B. The micromorphology of the aggregates and networks of gels is strongly dependent on the gel concentration, except for Pyb-0-B, and on the nature of the gelated solvent.

The xerogel morphology of Pyb-0-B in 1-octanol is formed by entangled nanotubes (Fig. 5a and b) with outer diameters in the range of 80–125 nm for the gels at 10% w/w and inner diameters around 3 nm, while in at a lower gelation concentration (2.5% w/w) two different sizes have been observed (30–40 and 80–100 nm). Interestingly, the gel in 1-octanol of this non-mesomorphic compound shows a lamellar structure, as revealed by the XRD of the bulk, with multiple periodic reflections (Fig. 6a); this is in fact similar to the molecular organization reported for the SmCP mesophase. In this case, the measured layer spacing by XRD (106 Å) is larger than the molecular length of the gelator (68 Å). This difference in layer spacing can be explained by the formation of a tilted bilayer in which two molecules are arranged in an antiparallel or parallel fashion and partially interdigitated through interacting pyrene units (estimated value: 126 Å) (Fig. 6b), which is in accordance with the observed excimeric emission. Interestingly, Pyb-0-B has a strong tendency to form nanotubes and the formation of this tubular structure has also been detected by TEM at lower concentrations (0.1% w/w) (Fig. 5i), showing outer diameters around 30 nm (Fig. 6c). As can be seen from the TEM images, all these nanotubes exhibit beveled ends with measured walls in the range of 10 nm. This is in accordance with the layer spacing measured by XRD and indicates that the nanotube walls are formed by a single bilayer.

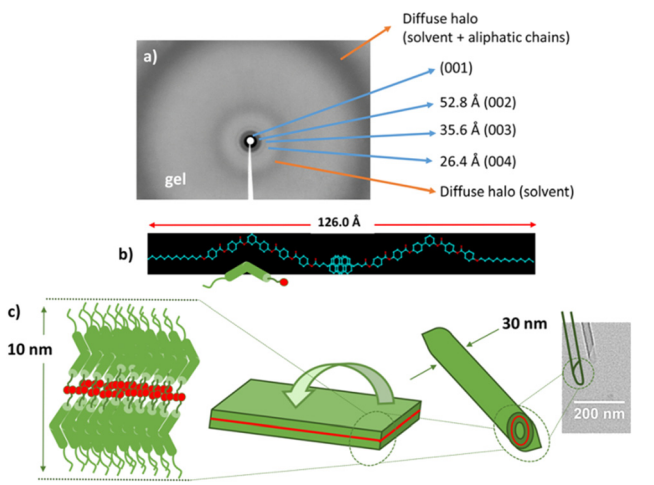

Fig. 6 XRD pattern of Pyb-0-B gel in 1-octanol (10% w/w) (a). Representation of the proposed structural repeating unit forming the gel Pyb-0-B and its theoretical molecular length (b), and schematic representation (c) proposed for the self-assembling tubular formation process (an antiparallel or parallel arrangement of molecules could be proposed).

These self-assembled nanotubes are indeed new forms of soft matter nanotubes (SMNTs); the latter is a current challenging topic in the area of materials chemistry.[109–112] In this case, by using bent-core molecules without hydrophilic and hydrophobic segments, well-defined nanotubes can be easily obtained.

For compound Pyb-11-B in 1-octanol, the morphology of the aggregates varies with the concentration of gelator, noting at the highest concentration (10% w/w) large sheets that fold (Fig. 5c), while at the minimum concentration (0.3% w/w) long flat ribbons are observed (Fig. 5d). The XRD study of the gel has demonstrated that the sheets exhibit a defined crystalline structure, with multiple reflections at small and wide angles and without a lamellar order. TEM studies of the aggregates, produced below the critical gelation concentration (0.1% w/w), showed that nanobelts (w: 100–400 nm) are formed by aggregation of initial nanofibers (w: 30 nm) (Fig. 5j).

Concerning the organogels of PybN-11-B, both soft materials gelling 1-octanol and chlorobenzene have been evaluated, which demonstrate that the morphology of the aggregates of the gel network depends on the solvent. When chlorobenzene is used, compact nanofibers (Fig. 5f) with a crystalline order can be observed (Fig. S11c, ESI†). On the other hand, using 1-octanol as a solvent, laminar structures appear creased and entangled, giving rise to balls (Fig. 5e). In this case, a liquid crystalline-like lamellar organization has been determined again by XRD (see Fig. S11a and b, ESI†), with a layer spacing (99.5 Å) larger than the molecular length (83.9 Å); this suggests a tilted bilayer order, favouring excimer pyrene–pyrene interactions.

Finally, for Pyb-11-C, self-assembled morphologies in the gels could not be clearly identified by SEM (Fig. 5g–h); however, TEM investigations suggest the presence of sheets with a high tendency for aggregation (Fig. 5k). The XRD studies of these gels have shown a lamellar structure for the aggregates, very similar to the molecular assembly in the liquid crystal phase of this compound. However, a larger layer spacing (61.6 Å) (Fig. S11d, ESI†) was found here, suggesting similar molecular organization in both supramolecular materials, both allowing for excimer formation.

Comparing the gels based on Pyb-11-C with a rod-core and those of its isomer Pyb-11-B with a bent-core, it can be concluded that while both compounds provide fluorescent gels, the non-linear structure affects the wavelength of the emitted light and it does not favour the formation of excimeric emission. Thus, Pyb-11-B based gels represent a rare example of pyrene-based ones with monomeric emission, supporting the high trends of its pyrene units to disperse in pristine, liquid crystal and gel, which condition weak intermolecular interactions.

Conclusions

The supramolecular abilities of five bent-shaped molecules, which incorporate pyrene moieties, were investigated, aiming at promoting both bent-core liquid crystalline phases and

 This journal is © The Royal Society of Chemistry 2022

Published on 29 Julai 2022. Downloaded on 30/01/2026 1:59:07 PTG.

supramolecular gels. Interestingly, by changing the number of 1-pyrenebutyrate units (1 or 2) and/or the presence or absence of a long and flexible linker between the bent-core structure and the pyrene motif, a variety of supramolecular materials can be achieved; the resulting properties depend on the molecular design, unveiling a synergistic and versatile 'tandem' of the bi-functional system in supramolecular functional materials chemistry.

The bent-core and pyrene combination limits the formation of mesophases as only compounds with a long spacer between them lead to monotropic columnar mesophases, interestingly around room temperature and with a glass transition, leading to a glassy mesophase-like organization. However, this tandem is more effective on solvent-mediated self-assembly, as either attractive nanoaggregates or gelation in certain organic solvents, even without amide bonds, is promoted as an alternative to liquid crystals. Molecular aggregations afford fibrillar and tubular morphologies through a liquid-crystalline-like lamellar organization of the molecules, with formation of beveled nanotubes built by a single bilayer.

In the absence of strong supramolecular interactions, long hydrocarbon spacers connecting bent-core and pyrene structures seem to allow the dilution of the pyrene fragment in the apolar environment, hindering either excimer or thermotropic liquid crystal formation, in contrast to linear isomers. Nevertheless, pyrene attractively transfers fluorescence properties always to all these supramolecular materials with quantum yields in the condensed phases of up to 60%.

Based on all these results and considering the singular design and functional potentials of these two structural motifs, the combination of bent-core and pyrene units opens broad and innovative research possibilities for challenging functional materials to explore. Using pyrene-bent core-based building blocks, a number of self-assembled materials which display BCLC-like features at room temperature, to form gels and nanoaggregates including tubular architectures, can be certainly proposed. Nevertheless, further opportunities, so far unexplored for this sort of molecules, are envisaged; this includes vibrant research fields such as optics, optoelectronic and molecular electronics.

Author contributions

The manuscript was written through contributions of all authors. All authors have given approval to the final version of the manuscript.

Conflicts of interest

There are no conflicts to declare.

Acknowledgements

The authors from INMA greatly appreciate financial support from projects of the Spanish Government PGC2018-093761-B-C31 [MCIU/AEI/FEDER, UE] and MAT2015-66208-C3-1 [MINECO/FEDER, UE], the Gobierno de Aragón/FEDER (research group E47_20R) and the JAE.PREDOC-CSIC (M. M.-A.) fellowship program. Thanks are given to the nuclear magnetic resonance, mass spectrometry, and thermal analysis services of the INMA (Univ. Zaragoza-CSIC), the LMA (Univ. Zaragoza) for TEM images and Servicio General de Apoyo a la Investigación-SAI (Univ. Zaragoza) for SEM images. The work at IMDEA was supported by the Spanish Government (MINECO-FEDER project CTQ2017-87054, MICINN project CEX2020-001039-S) and by the Campus of International Excellence (CEI) UAM+CSIC. We thank H. Bolink, Valencia, for access to the integrating sphere.

Notes and references

1 J. B. Birks and L. G. Christophorou, *Spectrochimica Acta*, 1963, **19**, 401–410.
2 F. M. Winnik, *Chem. Rev.*, 1993, **93**, 587–614.
3 T. M. Figueira-Duarte and K. Müllen, *Chem. Rev.*, 2011, **111**, 7260–7314.
4 S. M. M. Reddy, P. Dorishetty, G. Augustine, A. P. Deshpande, N. Ayyadurai and G. Shanmugam, *Langmuir*, 2017, **33**, 13504–13514.
5 S. Yang, Q. Liu, J. Ren and S. Ling, *Giant*, 2021, **5**, 100044.
6 M. El Idrissi, S. J. Teat, P. F. X. Corvini, M. J. Paterson, S. J. Dalgarno and P. Shahgaldian, *Chem. Commun.*, 2017, **53**, 1973–1976.
7 Y. Wu, H. Fan, C. Yang and L. Zhang, *Colloids Surf., A*, 2020, **585**, 124111.
8 M. Garrido, E. Martínez-Periñán, J. Calbo, L. Rodríguez-Pérez, J. Aragó, E. Lorenzo, E. Ortí, N. Martín and M. Á. Herranz, *J. Mater. Chem. C*, 2021, **9**, 10944–10951.
9 X. Bai, Y. Jiang, G. Zhao, J. Jiang, C. Yuan and M. Liu, *Soft Matter*, 2021, **17**, 4328–4334.
10 K. Kalyanasundaram and J. K. Thomas, *J. Am. Chem. Soc.*, 1977, **99**, 2039–2044.
11 P.-P. He, X.-D. Li, L. Wang and H. Wang, *Acc. Chem. Res.*, 2019, **52**, 367–378.
12 A. Méndez-Ardoy, A. Bayón-Fernández, Z. Yu, C. Abell, J. R. Granja and J. Montenegro, *Angew. Chem., Int. Ed.*, 2020, **59**, 6902–6908.
13 A. O. Ba-Salem and J. Duhamel, *Langmuir*, 2021, **37**, 6069–6079.
14 Y.-X. Li, L. Xu, S.-M. Kang, L. Zhou, N. Liu and Z.-Q. Wu, *Angew. Chem., Int. Ed.*, 2021, **60**, 7174–7179.
15 C. Madhu, B. Roy, P. Makam and T. Govindaraju, *Chem. Commun.*, 2018, **54**, 2280–2283.
16 D. Niu, Y. Jiang, L. Ji, G. Ouyang and M. Liu, *Angew. Chem., Int. Ed.*, 2019, **58**, 5946–5950.
17 Q. Wang, Q. Zhang, Q.-W. Zhang, X. Li, C.-X. Zhao, T.-Y. Xu, D.-H. Qu and H. Tian, *Nat. Commun.*, 2020, **11**, 158.
18 M. Pan, R. Zhao, B. Zhao and J. Deng, *Macromolecules*, 2021, **54**, 5043–5052.
19 J. H. van Esch and B. L. Feringa, *Angew. Chem., Int. Ed.*, 2000, **39**, 2263–2266.

Published on 29 Julai 2022. Downloaded on 30/01/2026 1:59:07 PTG.

20 N. M. Sangeetha and U. Maitra, *Chem. Soc. Rev.*, 2005, **34**, 821–836.
21 M. George and R. G. Weiss, *Acc. Chem. Res.*, 2006, **39**, 489–497.
22 S. Panja and D. J. Adams, *Chem. Soc. Rev.*, 2021, **50**, 5165–5200.
23 S. S. Babu, V. K. Praveen and A. Ajayaghosh, *Chem. Rev.*, 2014, **114**, 1973–2129.
24 S. Ghosh, V. K. Praveen and A. Ajayaghosh, *Annu. Rev. Mater. Res.*, 2016, **46**, 235–262.
25 E.-K. Fleischmann and R. Zentel, *Angew. Chem., Int. Ed.*, 2013, **52**, 8810–8827.
26 T. Kato, J. Uchida, T. Ichikawa and T. Sakamoto, *Angew. Chem., Int. Ed.*, 2018, **57**, 4355–4371.
27 T. Kato, M. Gupta, D. Yamaguchi, K. P. Gan and M. Nakayama, *Bull. Chem. Soc. Jpn.*, 2021, **94**, 357–376.
28 A. Hayer, V. de Halleux, A. Köhler, A. El-Garoughy, E. W. Meijer, J. Barberá, J. Tant, J. Levin, M. Lehmann, J. Gierschner, J. Cornil and Y. H. Geerts, *J. Phys. Chem. B*, 2006, **110**, 7653–7659.
29 K. P. Gan, M. Yoshio and T. Kato, *J. Mater. Chem. C*, 2016, **4**, 5073–5080.
30 Y. Sagara, C. Weder and N. Tamaoki, *Chem. Mater.*, 2017, **29**, 6145–6152.
31 M. Park, D.-G. Kang, Y.-J. Choi, W.-J. Yoon, J. Koo, S.-H. Park, S. Ahn and K.-U. Jeong, *Chem. – Eur. J.*, 2018, **24**, 9015–9021.
32 H. Anetai, K. Sambe, T. Takeda, N. Hoshino and T. Akutagawa, *Chem. – Eur. J.*, 2019, **25**, 11233–11239.
33 S. Irla, M. Pruthvi, V. A. Raghunathan and S. Kumar, *Dyes Pigm.*, 2021, **194**, 109574.
34 B. Yao, G. Zhao, H. Wu, C. Mo, Z. Meng, C. Luo, S. Wang, T. Chen, Y. Fu, Y. Chen and P. Lin, *J. Lumin.*, 2021, **239**, 118329.
35 T. M. S. K. Pathiranage, Z. Ma, C. M. Udamulle Gedara, X. Pan, Y. Lee, E. D. Gomez, M. C. Biewer, K. Matyjaszewski and M. C. Stefan, *ACS Omega*, 2021, **6**, 27325–27334.
36 B. Yao, Z. Huang, P. Lin, L. Li, S. Wang, G. Gong, Y. Chen, L. Dong, X. Wang and Y. Zang, *Liq. Cryst.*, 2021, **48**, 1087–1094.
37 R. Walker, M. Majewska, D. Pociecha, A. Makal, J. M. Storey, E. Gorecka and C. T. Imrie, *Chem. Phys. Chem.*, 2021, **22**, 461–470.
38 B. A. G. Lamers, M. H. C. van Son, F. V. de Graaf, B. W. L. van den Bersselaar, B. F. M. de Waal, K. Komatsu, H. Sato, T. Aida, J. A. Berrocal, A. R. A. Palmans, G. Vantomme, S. C. J. Meskers and E. W. Meijer, *Mater. Horizons*, 2022, **9**, 294–302.
39 J. J. van Gorp, J. A. J. M. Vekemans and E. W. Meijer, *J. Am. Chem. Soc.*, 2002, **124**, 14759–14769.
40 S. Yagai, T. Kinoshita, M. Higashi, K. Kishikawa, T. Nakanishi, T. Karatsu and A. Kitamura, *J. Am. Chem. Soc.*, 2007, **129**, 13277–13287.
41 K. Takashi and T. Kana, *Chem. Lett.*, 2009, **38**, 634–639.
42 S. Diring, F. Camerel, B. Donnio, T. Dintzer, S. Toffanin, R. Capelli, M. Muccini and R. Ziessel, *J. Am. Chem. Soc.*, 2009, **131**, 18177–18185.
43 F. Aparicio, F. García and L. Sánchez, *Chem. – Eur. J.*, 2013, **19**, 3239–3248.
44 N. Saito, K. Kanie, M. Matsubara, A. Muramatsu and M. Yamaguchi, *J. Am. Chem. Soc.*, 2015, **137**, 6594–6601.
45 D. Görl, B. Soberats, S. Herbst, V. Stepanenko and F. Würthner, *Chem. Sci.*, 2016, **7**, 6786–6790.
46 B. Pradhan, V. M. Vaisakh, G. G. Nair, D. S. S. Rao, S. K. Prasad and A. A. Sudhakar, *Chem. – Eur. J.*, 2016, **22**, 17843–17856.
47 A. P. Sivadas, D. S. S. Rao, N. S. S. Kumar, D. D. Prabhu, S. Varghese, C. N. Ramachandran, R. M. Ongungal, S. Krishna Prasad and S. Das, *J. Phys. Chem. B*, 2017, **121**, 1922–1929.
48 M. Castillo-Vallés, A. Martínez-Bueno, R. Giménez, T. Sierra and M. B. Ros, *J. Mater. Chem. C*, 2019, **7**, 14454–14470.
49 T. Niori, T. Sekine, J. Watanabe, T. Furukawa and H. Takezoe, *J. Mater. Chem.*, 1996, **6**, 1231–1233.
50 R. A. Reddy and C. Tschierske, *J. Mater. Chem.*, 2006, **16**, 907–961.
51 H. Takezoe and Y. Takanishi, *Jpn. J. Appl. Phys.*, 2006, **45**, 597–625.
52 A. Eremin and A. Jákli, *Soft Matter*, 2013, **9**, 615–637.
53 C. Tschierske, *Angew. Chem., Int. Ed.*, 2013, **52**, 8828–8878.
54 In *Handbook of Liquid Crystals*, ed. J. W. Goodby, P. J. Collings, T. Kato, C. Tschierske, H. Gleeson and P. Raynes, Wiley-VCH, Weinheim, 2014.
55 C. Tschierske and G. Ungar, *Chem. Phys. Chem.*, 2016, **17**, 9–26.
56 H. Takezoe, *Mol. Cryst. Liq. Cryst.*, 2017, **646**, 46–65.
57 J. Liu, S. Shadpour, M. E. Prévôt, M. Chirgwin, A. Nemati, E. Hegmann, R. P. Lemieux and T. Hegmann, *ACS Nano*, 2021, **15**, 7249–7270.
58 J. Etxebarria and M. B. Ros, *J. Mater. Chem.*, 2008, **18**, 2919–2926.
59 M. Martínez-Abadía, R. Giménez and M. B. Ros, *Adv. Mater.*, 2018, **30**, 1704161.
60 K. I. Shivakumar, D. Pociecha, J. Szczytko, S. Kapuściński, H. Monobe and P. Kaszyński, *J. Mater. Chem. C*, 2020, **8**, 1083–1088.
61 W. Park and D. K. Yoon, *Crystals*, 2020, **10**, 675.
62 R. Deb, R. K. Nath, M. K. Paul, N. V. S. Rao, F. Tuluri, Y. Shen, R. Shao, D. Chen, C. Zhu, I. I. Smalyukh and N. A. Clark, *J. Mater. Chem.*, 2010, **20**, 7332–7336.
63 R. Deb, A. R. Laskar, D. D. Sarkar, G. Mohiuddin, N. Chakraborty, S. Ghosh, D. S. Shankar Rao and N. V. S. Rao, *CrystEngComm*, 2013, **15**, 10510–10521.
64 R. Deb, M. Oneill, N. V. S. Rao, N. A. Clark and I. I. Smalyukh, *Chem. Phys. Chem.*, 2014, **16**, 243–255.
65 M. K. Paul, P. Paul, S. K. Saha and S. Choudhury, *J. Mol. Liq.*, 2014, **197**, 226–235.
66 R. Deb, M. Oneill, N. V. S. Rao, N. A. Clark and I. I. Smalyukh, *Chem. Phys. Chem.*, 2015, **16**, 243–255.
67 M. Martinez-Abadia, B. Robles-Hernandez, B. Villacampa, M. R. de la Fuente, R. Gimenez and M. B. Ros, *J. Mater. Chem. C*, 2015, **3**, 3038–3048.
68 M. Martinez-Abadia, S. Varghese, B. Milian-Medina, J. Gierschner, R. Gimenez and M. B. Ros, *Phys. Chem. Chem. Phys.*, 2015, **17**, 11715–11724.
69 M. Martínez-Abadía, B. Robles-Hernández, M. R. de la Fuente, R. Giménez and M. B. Ros, *Adv. Mater.*, 2016, **28**, 6586–6591.

This journal is © The Royal Society of Chemistry 2022

Published on 29 Julai 2022. Downloaded on 30/01/2026 1:59:07 PTG.

70 M. Martínez-Abadía, S. Varghese, P. Romero, J. Gierschner, R. Giménez and M. B. Ros, *Adv. Opt. Mater.*, 2017, **5**, 1600860.
71 K. V. Le, H. Takezoe and F. Araoka, *Adv. Mater.*, 2017, **29**, 1602737.
72 W. Lewandowski, N. Vaupotič, D. Pociecha, E. Górecka and L. M. Liz-Marzán, *Adv. Mater.*, 2020, **32**, 1905591.
73 K. Ariga, T. Mori, T. Kitao and T. Uemura, *Adv. Mater.*, 2020, **32**, 1905657.
74 N. Sebastián, N. Gimeno, J. Vergara, D. O. López, J. L. Serrano, C. L. Folcia, M. R. de la Fuente and M. B. Ros, *J. Mater. Chem. C*, 2014, **2**, 4027–4036.
75 N. Gimeno, J. Vergara, M. Cano, J. Luis Serrano, M. Blanca Ros, J. Ortega, C. L. Folcia, S. Rodriguez-Conde, G. Sanz-Enguita and J. Etxebarria, *Chem. Mater.*, 2013, **25**, 286–296.
76 M. Castillo-Vallés, M. Cano, A. Bermejo-Sanz, N. Gimeno and M. B. Ros, *J. Mater. Chem. C*, 2020, **8**, 1998–2007.
77 C. Keith, R. A. Reddy, A. Hauser, U. Baumeister and C. Tschierske, *J. Am. Chem. Soc.*, 2006, **128**, 3051–3066.
78 W.-H. Chen, W.-T. Chuang, U. S. Jeng, H.-S. Sheu and H.-C. Lin, *J. Am. Chem. Soc.*, 2011, **133**, 15674–15685.
79 R. A. Reddy, C. Zhu, R. Shao, E. Korblova, T. Gong, Y. Shen, E. Garcia, M. A. Glaser, J. E. Maclennan, D. M. Walba and N. A. Clark, *Science*, 2011, **332**, 72–77.
80 E. Westphal, H. Gallardo, G. F. Caramori, N. Sebastián, M.-G. Tamba, A. Eremin, S. Kawauchi, M. Prehm and C. Tschierske, *Chem. – Eur. J.*, 2016, **22**, 8181–8197.
81 E. Westphal, H. Gallardo, N. Sebastián, A. Eremin, M. Prehm, M. Alaasar and C. Tschierske, *J. Mater. Chem. C*, 2019, **7**, 3064–3081.
82 J. Vergara, J. Barberá, J. L. Serrano, M. B. Ros, N. Sebastián, R. de la Fuente, D. O. López, G. Fernández, L. Sánchez and N. Martín, *Angew. Chem., Int. Ed.*, 2011, **50**, 12523–12528.
83 M. Pfletscher, S. Hölscher, C. Wölper, M. Mezger and M. Giese, *Chem. Mater.*, 2017, **29**, 8462–8471.
84 M. Cano, A. Sánchez-Ferrer, J. L. Serrano, N. Gimeno and M. B. Ros, *Angew. Chem., Int. Ed.*, 2014, **53**, 13449–13453.
85 M. Castillo-Vallés, P. Romero, V. Sebastián and M. B. Ros, *Nanoscale Adv.*, 2021, **3**, 1682–1689.
86 D. Shen, A. Pegenau, S. Diele, I. Wirth and C. Tschierske, *J. Am. Chem. Soc.*, 2000, **122**, 1593–1601.
87 I. C. Pintre, N. Gimeno, J. L. Serrano, M. B. Ros, I. Alonso, C. L. Folcia, J. Ortega and J. Etxebarria, *J. Mater. Chem.*, 2007, **17**, 2219–2227.
88 The S0 → S1 is hardly visible due to the low oscillator strength, f around 0.002, see R. S. Becker, I. S. Singh and E. A. Jackson, *J. Chem. Phys.*, 1963, **38**, 2144–2171.
89 In deaerated solution, the quantum yields are around 30%; see W. R. Dawson and M. W. Windsor, *J. Phys. Chem.*, 1968, **72**, 3251–3260.
90 Birks suggested to define an excimer as ''a molecular dimer or stoichiometric complex which is associated in an excited electronic state and which is dissociative (*i.e.*, dissociates in the absence of external restraints) in its electronic ground state''; see J. B. Birks, in *The Exciplex*, ed. M. Gordon and W. R. Ware, Academic Press, New York, 1975, p. 39.
91 S. K. Behera, S. Y. Park and J. Gierschner, *Angew. Chem., Int. Ed.*, 2021, **60**, 22624–22638.
92 S. Farid, P. A. Martic, R. C. Daly, D. R. Thompson, D. P. Specht, S. E. Hartman and J. L. R. Williams, *Pure Appl. Chem.*, 1979, **51**, 241.
93 A. Warshel and E. Huler, *Chem. Phys.*, 1974, **6**, 463–468.
94 F. Hirayama, *J. Chem. Phys.*, 1965, **42**, 3163–3171.
95 J. Gierschner, H.-G. Mack, D. Oelkrug, I. Waldner and H. Rau, *J. Phys. Chem. A*, 2004, **108**, 257–263.
96 S. Reiter, M. K. Roos and R. de Vivie-Riedle, *ChemPhotoChem*, 2019, **3**, 881–888.
97 For an ideal side-by-side arrangement of a dimer, the simple electronic exciton model predicts a zero oscillator strength *f*; static and dynamic symmetry breaking then gives rise to little, but non-zero *f*. The resulting f is directly proportional to k_F *via* the Strickler-Berg relation; see S. J. Strickler and R. A. Berg, *J. Chem. Phys.*, 1962, **37**, 814–822.
98 J. Gierschner, J. Shi, B. Milián-Medina, D. Roca-Sanjuán, S. Varghese and S. Park, *Adv. Opt. Mater.*, 2021, **9**, 2002251.
99 R. Katoh, K. Suzuki, A. Furube, M. Kotani and K. Tokumaru, *J. Phys. Chem. C*, 2009, **113**, 2961–2965.
100 While Pyb-11-*B*-11-Pyb (*i.e.* with long spacers) exhibits a k_r of 9.6×10^6 s^{-1}; a smaller k_r (6.1×10^6 s^{-1}) is found in the corresponding compound with short spacers, Pyb-0-*B*-0-Pyb. This may be due to the fact that the short spacers enforce a slightly different π–π-stacking, which changes the resulting oscillator strength of the emitting state.
101 J. Shi, L. E. Aguilar Suarez, S.-J. Yoon, S. Varghese, C. Serpa, S. Y. Park, L. Lüer, D. Roca-Sanjuán, B. Milián-Medina and J. Gierschner, *J. Phys. Chem. C*, 2017, **121**, 23166–23183.
102 It is noted that also reabsorption contributes to non-exponential lifetimes in molecular solids; this was however largely avoided in the experiments by effectively reducing light penetration, see *e.g.* ref. 97.
103 K. Lalitha and S. Nagarajan, *J. Mater. Chem. B*, 2015, **3**, 5690–5701.
104 D. Kraskouskaya, M. Bancerz, H. S. Soor, J. E. Gardiner and P. T. Gunning, *J. Am. Chem. Soc.*, 2014, **136**, 1234–1237.
105 N. Prigyai, S. Chanmungkalakul, S. Thanyalax, M. Sukwattanasinitt and V. Ervithayasuporn, *Materials Adv.*, 2020, **1**, 3358–3368.
106 S. Mondal, P. Bairi, S. Das and A. K. Nandi, *J. Mater. Chem. A*, 2019, **7**, 381–392.
107 D. Chen, C. Zhu, H. Wang, J. E. Maclennan, M. A. Glaser, E. Korblova, D. M. Walba, J. A. Rego, E. A. Soto-Bustamante and N. A. Clark, *Soft Matter*, 2013, **9**, 462–471.
108 A. Zep, M. Salamonczyk, N. Vaupotič, D. Pociecha and E. Gorecka, *Chem. Commun.*, 2013, **49**, 3119–3121.
109 T. G. Barclay, K. Constantopoulos and J. Matisons, *Chem. Rev.*, 2014, **114**, 10217–10291.
110 A. Nitti, A. Pacini and D. Pasini, *Nanomaterials*, 2017, **7**, 167.
111 V. Novotná, V. Hamplová, L. Lejček, D. Pociecha, M. Cigl, L. Fekete, M. Glogarová, L. Bednárová, P. W. Majewski and E. Gorecka, *Nanoscale Adv.*, 2019, **1**, 2835–2839.
112 T. Shimizu, W. Ding and N. Kameta, *Chem. Rev.*, 2020, **120**, 2347–2407.